Geology

Origin of basalt fire-fountain eruptions on Earth versus the Moon

Malcolm J. Rutherford and Paolo Papale

Email alerting services	click www.gsapubs.org/cgi/alerts to receive free e-mail alerts when new articles cite this article
Subscribe	click www.gsapubs.org/subscriptions/ to subscribe to Geology
Permission request	click http://www.geosociety.org/pubs/copyrt.htm#gsa to contact GSA

Notes

THE
GEOLOGICAL
SOCIETY
OF AMERICA

Origin of basalt fire-fountain eruptions on Earth versus the Moon

Malcolm J. Rutherford[1]* and Paolo Papale[2]

[1]Department of Geological Sciences, Brown University, Providence, Rhode Island 02912, USA
[2]Istituto Nazionale di Geofisica e Vulcanologia, Sezione di Pisa, 56126 Pisa, Italy

ABSTRACT

Fire-fountain eruptions of basaltic magma occur on Earth at centers such as Kilauea (Hawaii), and deposits from apparently similar eruptions have been found on the lunar surface. The driving force for terrestrial fire-fountain eruptions is the exsolution of dissolved CO_2 based on gases dissolved in melt inclusions trapped in olivine phenocrysts and the relatively high oxidation state of these magmas. Gases released at the vent show that SO_2, and eventually H_2O, are partitioned into the CO_2-rich gas, adding to the gas volume. In contrast, analytical and experimental studies of lunar samples indicate that the gas phase responsible for driving the lunar eruptions was CO-rich and produced by the oxidation of C (graphite) carried in the slowly ascending low-fO_2 basalt. The graphite oxidation occurs when the pressure in the ascending lunar magma reaches that of the graphite-gas reaction surface (40 ± 1 MPa or ~8 km depth for the Apollo 17 orange-glass magma). As graphite is oxidized, some FeO is reduced, potentially forming a Fe-rich metal phase, and Fe-rich metal spherules are present in beads in lunar glass deposits. Other gas species such as S, Cl, and F partitioned variously into CO-rich lunar volcanic gas, and appear in surface coatings on the glass spherules. Modeling of the magma flow from 8 km depth to the lunar surface shows that the gas bubble volume fraction (assuming initial C at 50–500 ppm levels) ranges from 0.5 to 0.8 at the surface, the exit velocity ranges from 15 to 35 m/s, and the low-viscosity magma fragments only as it erupts at the lunar surface.

INTRODUCTION

Basalt fire-fountain eruptions on Earth are a well-known end member in a range of volcanic eruption styles that extend from explosive gas-rich, fire-fountain events to extrusive lava flows. The fire-fountain eruptions of Kilauea (Hawaii) in 1959 (Eaton and Murata, 1960) and 1983 (Wolfe et al., 1987) are well-known examples of this eruption style. The main driving force for such eruptions is generally considered to be the exsolution and expansion of volatiles such as CO_2 and H_2O that are dissolved in the magma at depth, and released as the magma rises toward the surface (Gerlach and Graeber, 1985). CO_2, H_2O, and to a lesser extent SO_2 are degassed during Kilauea eruptions, and gas solubility data suggest that a CO_2-rich gas was present in the Kilauea magmas at depths of at least 20 km (Gerlach et al., 2002). Interestingly, we also have samples from what appear to be fire-fountain eruptions of basalt magma on the Moon, even though the lunar gravity is significantly lower and the pressure decrease in moving from a given depth to the surface is only one-sixth that of Earth. The lunar fire-fountain eruptions produced deposits of fine (<1 mm) glass spherules with primitive olivine-rich compositions. The glass compositions range from very TiO_2-rich (9–16 wt%) basalts such as those found in the >1-m-thick orange-glass deposit (Fig. 1) at the Apollo 17

(A17) site to very low-TiO_2 green glasses (Delano, 1986) such as those found on the surface at the A15 site. Other observations that must be considered in a viable eruption model include the following: (1) The picritic lunar magmas are usually phenocryst-free (Steele et al., 1992), although the A17 orange-glass deposit contains ~1 vol% euhedral, compositionally homogenous (Fo_{82}) olivine phenocrysts (Heiken et al., 1974). Therefore the eruptions were at or above the 1 atm liquidus temperatures (1400–1520 °C; Fogel and Rutherford, 1995) for these magmas. (2) Vesicles are present in the lunar glass spherules but are not abundant in contrast to the highly vesicular glasses in the deposits of Kilauea (Fig. 1B) and other terrestrial volcanoes (Heiken, 1972). (3) Cooling of the lunar glass spherules had to be very rapid in order to quench them to a glass, given their high liquidus temperatures (anhydrous) and very low viscosities compared to terrestrial basalts. However, many of the larger spherules in the lunar deposits are
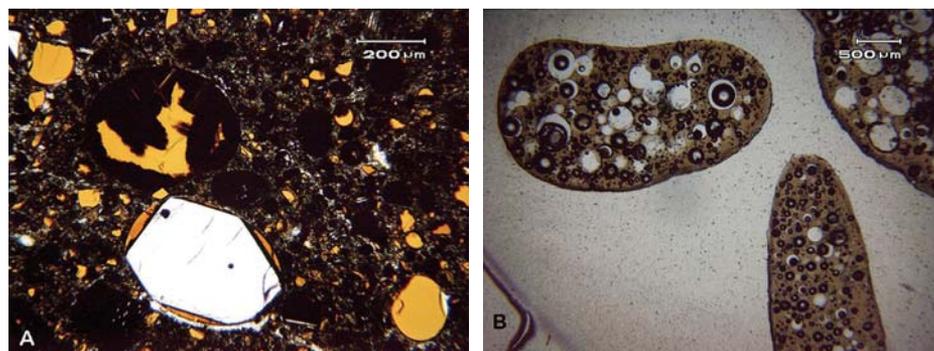

Figure 1. Optical photomicrographs. A: Thin section near top of A17 orange-glass deposit (74001/2 drill core) showing small and large beads and fragments making up the deposit. Glass beads are variably devitrified to a microcrystalline mixture of cryptocrystalline olivine and ilmenite (Weitz et al., 1999). Bead at center bottom contains a euhedral olivine microphenocryst that contains two metal spherules formed by graphite oxidation prior to growth of the phenocrysts. B: Thin section made from small (2–3 mm) rounded glass spherules erupted in the 1959 Kilauea Iki eruption. Olivine phenocrysts (<5 mm) are present in this basalt, and microlites occur in the beads. The high vesicle content of these beads dominates the internal texture compared to the lunar orange glass.

*E-mail: malcolm_rutherford@brown.edu.

a mix of acicular to fibrous crystals in a residual glass (Fig. 1); the imperfect quench has been attributed to the presence of hot volcanic gas erupted with the microspheres (Housley, 1978; Arndt and von Englehardt, 1987).

Initially, the lunar glass deposits were considered to be either volcanic or impact in origin, but as new evidence accumulated, it became clear that these glass deposits are of volcanic origin (Heiken et al., 1974; Delano, 1986). Glasses produced by impact commonly contain partially resorbed crystals and rock fragments of the target rocks, and these are lacking in the picritic glasses. The volcanic fire-fountain model for the picritic glasses also explains the very thin coating of volatile elements such as S, F, Cl, Na, and Pb (Meyer et al., 1975) on the glass spherules. While these elements were very likely components of the lunar volcanic gas generated in the eruption, the calculated vapor pressure of these elements at magmatic temperatures is <0.1 MPa, indicating they would not generate a gas phase in magmas below the lunar surface (Sato, 1976). Sato proposed a model involving the oxidation of graphite to produce a CO-rich volcanic gas in magma undergoing ascent that has since been generally validated (Fogel and Rutherford, 1995; Weitz et al., 1997). This paper compares the gas generation process in lunar versus terrestrial basalt magma systems, refines the model for gas formation on the Moon, and describes numerical, fluid dynamical simulations (Papale, 2001) of the A17 orange-glass magma ascent and eruption process using petrologic constraints. For comparison, we also present simulations of magma ascent for basalt fire-fountain eruptions on Earth, and highlight the differences in the fire-fountain process for the two bodies.

MECHANISMS OF GAS FORMATION IN BASALT MAGMA
Origin by Graphite Oxidation

On the Moon, the oxidation state of the mantle is relatively reduced ($fO_2 \approx$ QFM-4 log units; Sato, 1976) in comparison to Earth's upper mantle (QFM-2; Balhaus and Frost, 1994) where QFM-4 refers to the oxygen fugacity set by the quartz-fayalite-magnetite buffer minus 4 log units. At the low-fO_2 and low-pressure conditions of the lunar basalt source region (<2 GPa; Longhi, 1992), carbon is present as graphite rather than $CO + CO_2$ (Fig. 2). The generation of a volcanic gas by graphite oxidation occurs when a magma containing reduced carbon rises toward the surface. The process can be illustrated using an oxygen fugacity versus pressure plot for a near-liquidus temperature of the magma being considered (Fig. 2). In this plot, the graphite-gas curve is a constant-temperature slice through the graphite-gas surface in the C-O system, a surface where graphite is in equilibrium with a CO-CO_2 gas phase (+ melt). Below
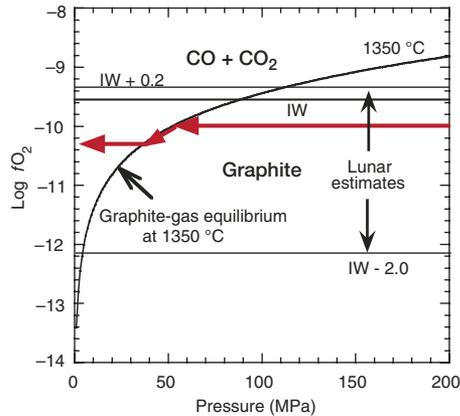

Figure 2. Plot of log oxygen fugacity versus pressure (both in MPa) illustrating an isothermal (1350 °C) section in the C-O system and how a graphite-bearing, low-fO_2 basalt (IW buffer conditions; IW = iron + wustite) would intersect the graphite-gas surface with decreasing pressure in a magma ascent. The pressure at which a CO-rich gas first forms is dependent on the intrinsic fO_2, a_{FeO}, and temperature of the basalt (Fogel and Rutherford, 1995). Assuming the basalt carries <2000 ppm C, the oxidation would be complete in a small pressure range beginning at 40 MPa (Nicholis and Rutherford, 2005).

the surface, graphite (diamond at very high pressures) is the stable C-bearing phase, and above it only the gas phase is stable. Magma produced in the lunar interior at pressures >40 MPa would ascend along a path of approximately constant oxidation state (arrow in Fig. 2). At a pressure depending on the fO_2 and the a_{FeO} in that magma, the P-fO_2 path would intersect the graphite-gas surface, and a gas phase would appear as graphite is oxidized. The oxidation would initially reduce any ferric iron present in the melt to FeO, and then ferrous iron would be reduced to Fe-metal. Reduction of higher valence states of chrome and titanium is also expected, and Ni and Co would enter the new Fe-rich metal preferentially (Weitz et al., 1999). The presence of FeNiCo-metal spherules in the picritic glasses and trapped inside the olivine microphenocrysts (Fig. 1) is convincing evidence that the graphite oxidation process did occur at depth in the lunar picritic magmas. The graphite abundance in the lunar picritic magmas is unlikely to have been more than a few hundred ppm based on the observed abundance of the Fe-metal (Sato, 1976; Fogel and Rutherford, 1995).

Weitz et al. (1997) used the compositions of Fe-metal spherules and coexisting melt (glass) to calculate a 22.5 MPa pressure (depth of 4 km) for the Fe + $1/2 O_2$ = FeO equilibrium in the A17 orange-glass magma. Recently, Nicholis and Rutherford (2005) reversibly simulated the reaction experimentally and determined that it

actually occurs at 40 MPa or 8 km depth; the increased depth estimate results from revisions in the melt a_{FeO} and the magma temperature. All graphite exposed to melt would oxidize at this pressure, oxidation-reduction kinetics permitting, and thus the entire CO_2-CO gas phase is generated at this depth for graphite abundances in the hundreds of ppm range. There is essentially no detectable (6 ppm) dissolved CO_3 or CO_2 in any of the picritic glasses (Saal et al., 2008), but none would be expected because the C-O solubility at 40 MPa and 1350 °C is very low (Fogel and Rutherford, 1995). Additionally, the picritic, melt-rich magmas would tend to degas during ascent to the lunar surface, losing C-O gas species initially dissolved in the melt. However, carbon has been detected in the volatile-element coatings on the glass spherules (McKay and Wentworth, 1992)—another confirmation of its role in the volcanic gas phase.

Wilson and Head (2003) suggest that the low-pressure regime generally thought to exist at the tip of a propagating dike carrying the picritic lunar basalts may have caused the oxidation of graphite to occur at even greater depths in the Moon as basalt dike flow was being initiated. If the graphite could be regularly brought to the low pressures at the crack (dike) tip, this mechanism could explain how the melt-filled dike became established. Here we consider the mechanism and dynamics of a steady-state eruption after a melt column is established.

Although this paper deals primarily with the generation of a CO-rich gas in the TiO_2-rich orange-glass magma, the petrologic evidence (glass beads with Fe-rich metal) indicates that the same process occurred in other lunar picritic magma eruptions (Fogel and Rutherford, 1995) and in most if not all effusive lunar basalt eruptions. The graphite in these magmas must have survived an oxidation process that would have tended to occur during convection in the lunar magma ocean (Longhi, 1992). We speculate that the ubiquitous Fe-rich metal in lunar highland rocks was produced in part by graphite oxidation during convection and crystallization in the lunar magma ocean.

Exsolution Origin of Gas Phase

While the C in the lunar interior is in the reduced form of graphite, available evidence suggests that it is oxidized and dissolved as C-O species in the melt of deep-seated terrestrial basalt magmas (Holloway and Blank, 1994). Oxidized C is consistent with the fact that mineral equilibria in terrestrial magmas show they are one to two log units of fO_2 more oxidized (Balhaus and Frost, 1994) than lunar basalts. Melt inclusions trapped in olivine phenocrysts in terrestrial basalts commonly contain dissolved CO_2 contents of up to 5000–7000 ppm (Hekinian et al., 2000; Gerlach

et al., 2002), indicating they were trapped at >20–30 km depth as phenocrysts grew in a relatively oxidized magma. A CO_2-rich magmatic gas phase is generated in these magmas when CO_2 saturation is reached during ascent-induced decompression, and CO_2 exsolution continues with additional decompression.

DYNAMICS OF LUNAR MAGMA ASCENT

Simulations of lunar picritic magma ascent from the point of graphite oxidation at depth to the surface using the "Conduit4" fluid dynamic code (Papale, 2001) show the physical characteristics of the A17 orange-glass eruption as a function of initial graphite content as well as other possible variables (e.g., feeder dike width). These explosive eruptions have been modeled in the past (Housley, 1978; Wilson and Head, 1981) but without the depth-of-gas-formation constraint and recent viscosity data. The Conduit4 code computes the steady-state, isothermal two-phase flow of gas and magma through a conduit in a lunar crust environment. Gas is formed at 8000 m (~40 MPa), is CO-rich (90%; Fogel and Rutherford, 1995), is at the orange-glass liquidus temperature of 1350 °C, and is homogenously distributed as small bubbles in the melt (bubble density = 10^{11} m^{-3}). The magma melt density is assumed constant at 3000 kg/m^3, and the melt viscosity, 10 Pa·s (calculated after Giordano and Dingwell, 2003), is also assumed constant, while the viscosity of the melt-gas mixture depends on the gas volume fraction (Papale, 2001). All the simulations are for flow through a vertical fracture (0.5–4 m wide × 8 km deep) with initial C contents of 50–2000 ppm, and CO/(CO + CO_2) = 0.9 by weight. Lunar gravity is one-sixth that on Earth. To compare the dynamics of lunar picritic magma flow with fire-fountain eruptions on Earth, a subset of simulations was done for a typical tholeiitic composition with the same fissure geometry. The input data and some relevant results are given in Tables DR1 and DR2 (see the GSA Data Repository[1]), and results are plotted in Figure 3.

The calculated initial gas volume and the gas volume at any point along the fissure (Fig. 3A) are directly proportional to the initial C (or H_2O-CO_2 for the tholeiite) content assumed for any dike width. However, all scenarios examined produce a significant increase in gas volume (and magma volume) in the final 2000 m of ascent to the surface. In a 2-m-wide dike,

---

[1]GSA Data Repository item 2009059, Table DR1 (results of numerical simulations of A17 orange-glass magma ascent in the lunar crust) and Table DR2 (results of numerical simulations of tholeiitic magma ascent on Earth), is available online at www.geosociety.org/pubs/ft2009.htm, or on request from editing@geosociety.org or Documents Secretary, GSA, P.O. Box 9140, Boulder, CO 80301, USA.
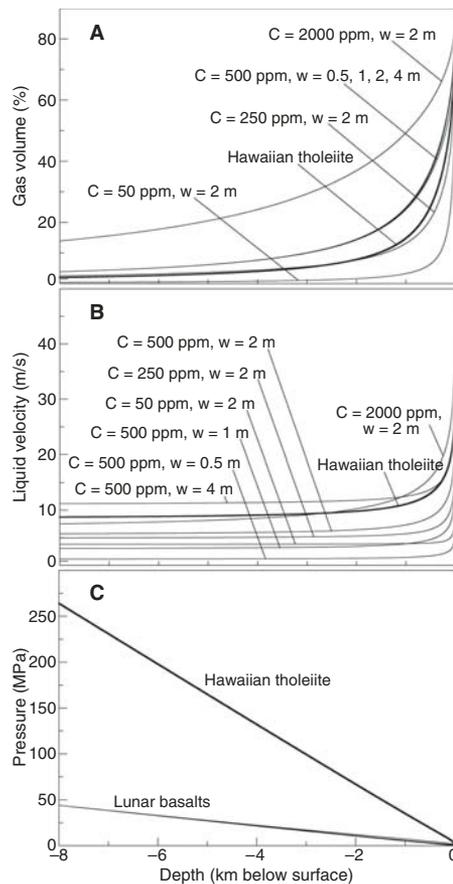

Figure 3. Results of the Conduit4 numerical simulation of A17 orange-glass magma flow from 8 km depth to the surface compared to a tholeiite magma (with 0.1 wt% H_2O and 1 wt% CO_2) ascent on Earth (see Table DR1). A: Gas volume for different amounts of graphite (C = 50–2000 ppm) and dike widths (w = 0.5–4 m). B: Liquid velocity for the same initial graphite contents and dike widths. C: Pressure in the conduit for the lunar cases (all equal within error) versus a Hawaiian tholeiite ascent over the same distance on Earth.

liquid velocities vary from 4.1 to 8.4 m/s at the fissure base, and from 10 to 46 m/s at the fissure exit for initial C contents of 50–2000 ppm. The exit gas volume ranges from 60% to 90% depending on the initial C content, and at this point the A17 orange-glass magma would consist of gas bubbles separated by thin walls of melt. Interestingly, the Conduit4 code indicates that the A17 magma would not meet the viscous-to-elastic transition (where magma fragmentation occurs; Papale, 1999) in the conduit in spite of the large acceleration near the fissure exit; this result stems from the very low mixture viscosity (~60 Pa·s) produced by the high temperature and unique liquid composition. Although the ambient surface pressure approaches zero (vacuum) on the Moon due to lack of an atmosphere, the calculated magma exit pressure is always greater than 0.1 MPa

(Table DR1). This is due to achievement of choked-flow conditions here, unavoidable on the Moon since the fast-flowing magma cannot equilibrate to the external pressure. In this situation, the liquid-gas mixture experiences a sudden additional decompression as it is erupted. Ductile fragmentation (Cashman et al., 2000) is therefore expected to occur at the vent as a consequence of massive gas expansion. The low magma viscosity, two orders of magnitude less than that of magmas erupting in terrestrial fire-fountain eruptions, would tend to prevent gas bubble entrapment in the liquid even after surface tension causes thin pieces of bubble wall to form melt spherules. This explains the generally gas-bubble-poor character of the lunar glass beads; the small size of the beads (<1 mm) is due to the high bubble volume (thin bubble walls) prior to eruption and fragmentation. Also, the bubble volumes calculated here for the lunar magma are minima because other species (S, Cl, H_2O) partitioned into the gas phase after it formed, although their amounts are not yet well known.

We note that posteruptive decompression due to flow choking near the vent will accelerate the magmatic mixture to supersonic velocities. Thus, the exit velocities described in this paper do not represent the maximum velocities achieved by the magma above the vent. According to the method proposed in Neri et al. (1998), maximum theoretical velocities immediately above the vent for the terrestrial eruptions simulated here can be estimated at ~130 m/s. For the lunar case, rapid cooling due to extremely low ambient temperature implies maximum velocities that were significantly less than the theoretical maximum, estimated in the range 50–100 m/s.

Figure 3 shows that in spite of big differences in gravity and in magma composition as well as in the mechanisms of gas phase generation between lunar and terrestrial basalt fire-fountain eruptions, their dynamics are quite similar, and apart from minor variations, the conditions of the magmatic mixture emerging at the Moon's and Earth's surface largely overlap. We suggest that the formation of the glass beads on the Moon occurs by ductile fragmentation above the vent, triggered by the combined effects of low magma viscosity and zero ambient pressure. The large bubble volume and low magma viscosity produced thin bubble walls and relatively small melt beads during fragmentation. In contrast, the higher viscosity of an ascending terrestrial basalt (a product of its composition and temperature) causes fragmentation below Earth's surface at a relatively lower bubble volume and produces generally larger glass spherules, which continue to experience bubble formation and growth with little or no bubble loss.

REFERENCES CITED

Arndt, J., and Von Engelhardt, W., 1987, Formation of Apollo 17 orange and black glass beads: Proceedings of the 17th Lunar and Planetary Science Conference: Journal of Geophysical Research, v. 92, no. B4, p. E372–E376, doi: 10.1029/JB092iB04p0E372.

Balhaus, C., and Frost, R.B., 1994, The generation of oxidized CO_2-bearing basaltic melts from reduced CH_4-bearing upper mantle sources: Geochimica et Cosmochimica Acta, v. 58, p. 4931–4940, doi: 10.1016/0016-7037(94)90222-4.

Cashman, K.V., Sturtevant, B., Papale, P., and Navon, O., 2000, Magmatic fragmentation, *in* Sigurdsson, H., et al., eds., Encyclopedia of volcanoes: Orlando, Florida, Academic Press, p. 421–430.

Delano, J.W., 1986, Pristine lunar glasses: Criteria, data and implications: Proceedings of 16th Lunar and Planetary Science Conference, p. D201–D213.

Eaton, J.P., and Murata, K.J., 1960, How volcanoes grow: Science, v. 132, p. 925–938, doi: 10.1126/science.132.3432.925.

Fogel, R.A., and Rutherford, M.J., 1995, Magmatic volatiles in primitive lunar glasses, I: FTIR and EPMA analyses of Apollo 15 green and yellow glasses and revision of the volatile-assisted fire-fountain theory: Geochimica et Cosmochimica Acta, v. 59, p. 201–215, doi: 10.1016/0016-7037 (94)00377-X.

Gerlach, T.M., and Graeber, E.J., 1985, Volatile budget of Kilauea volcano: Nature, v. 313, p. 273–277, doi: 10.1038/313273a0.

Gerlach, T.M., McGee, K.A., Elias, T., Sutton, A.J., and Doukas, M.P., 2002, Carbon dioxide emission rate of Kilauea volcano: Implications for primary magma and the summit reservoir: Journal of Geophysical Research, v. 107, no. B9, p. 2189, doi: 10.1029/2001JB000407.

Giordano, D., and Dingwell, D.B., 2003, Non-Ahrenian multicomponent melt viscosity: A model: Earth and Planetary Science Letters, v. 208, p. 337–349, doi: 10.1016/S0012-821X (03)00042-6.

Heiken, G.H., 1972, Morphology and petrography of volcanic ashes: Geological Society of America Bulletin, v. 84, p. 455–488.

Heiken, G.H., McKay, D.S., and Brown, R.W., 1974, Lunar deposits of possible pyroclastic origin: Geochimica et Cosmochimica Acta, v. 38, p. 1703–1718, doi: 10.1016/0016-7037 (74)90187-2.

Hekinian, R., Pineau, F., Shilobreeva, S., Bideau, D., Gracia, E., and Javoy, M., 2000, Deep sea explosive activity on the Mid-Atlantic Ridge near 34°50′ N: Magma composition, vesicularity, and volatile content: Journal of Volcanology and Geothermal Research, v. 98, p. 49–77, doi: 10.1016/S0377-0273(99)00190-0.

Holloway, J.R., and Blank, J.G., 1994, Application of experimental results to C-O-H species in natural melts: Reviews in Mineralogy, v. 30, p. 187–230.

Housley, R.M., 1978, Modeling lunar volcanic eruptions: Proceedings of 9th Lunar and Planetary Science Conference, p. 1473–1484.

Longhi, J., 1992, Lunar petrology and petrogenesis of mare volcanics: Geochimica et Cosmochimica Acta, v. 56, p. 2235–2251, doi: 10.1016/0016-7037(92)90186-M.

McKay, D.S., and Wentworth, S.J., 1992, Morphology and composition of condensates on Apollo 17 orange and black glasses: LPI Technical Report 92-09, Part 1: Houston, Texas, Lunar and Planetary Institute, p. 31–36.

Meyer, C., McKay, D.S., Anderson, D.H., and Butler, P., 1975, The source of sublimates on the Apollo 15 green and Apollo 17 orange glass samples: Proceedings of 6th Lunar and Planetary Science Conference, p. 1673–1699.

Neri, A., Papale, P., and Macedonio, G., 1998, The role of magma composition and water content in explosive eruptions, 2: Pyroclastic dispersion dynamics: Journal of Volcanology and Geothermal Research, v. 87, p. 95–115, doi: 10.1016/S0377-0273(98)00102-4.

Nicholis, M.G., and Rutherford, M.J., 2005, Pressure dependence of graphite-C-O phase equilibria and its role in lunar volcanism: Proceedings of 36th Lunar and Planetary Science Conference, abstract 1732.

Papale, P., 1999, Strain-induced magma fragmentation in explosive eruptions: Nature, v. 397, p. 425–428, doi: 10.1038/17109.

Papale, P., 2001, Dynamics of magma flow in volcanic conduits with variable fragmentation efficiency and nonequilibrium pumice degassing: Journal of Geophysical Research, v. 106, no. B6, p. 11,043–11,065, doi: 10.1029/2000JB900428.

Saal, A.E., Hauri, E.H., Lo Cassio, M., Van Orman, J.A., Rutherford, M.J., and Cooper, R.F., 2008, The volatile content of the lunar volcanic glasses: Evidence for the presence of water in the Moon's interior: Nature, v. 454, p. 192–195, doi: 10.1038/nature07047.

Sato, M., 1976, Oxygen fugacity and other thermochemical parameters of Apollo 17 high-Ti basalts and their implications on the reduction mechanism: Proceedings of 7th Lunar and Planetary Science Conference, p. 1323–1344.

Steele, A.M., Colson, R.O., Kortev, R.L., and Haskin, L.A., 1992, Apollo 15 green glass: Compositional distribution and petrogenesis: Geochimica et Cosmochimica Acta, v. 56, p. 4075–4090, doi: 10.1016/0016-7037(92)90017-D.

Weitz, C.M., Rutherford, M.J., and Head, J.W., 1997, Oxidation states and ascent history of the Apollo 17 volcanic beads as inferred from metal-glass equilibria: Geochimica et Cosmochimica Acta, v. 61, p. 2765–2775, doi: 10.1016/S0016-7037(97)00119-1.

Weitz, C.M., Rutherford, M.J., Head, J.W., and McKay, D.S., 1999, Ascent and eruption of a lunar high-titanium magma as inferred from petrology of the 74001/2 drill core: Meteoritics and Planetary Science, v. 34, p. 527–540.

Wilson, L., and Head, J.W., III, 1981, Ascent and eruption of basaltic magmas on the Earth and Moon: Journal of Geophysical Research, v. 86, no. B4, p. 2971–3001, doi: 10.1029/ JB086iB04p02971.

Wilson, L., and Head, J.W., III, 2003, Deep generation of magmatic gas on the Moon and implication for pyroclastic eruptions: Geophysical Research letters, v. 30, p. 1605–1609, doi: 10.1029/2002GL016082.

Wolfe, E.W., Garcis, M.O., Jackson, D.B., Koyagani, R.Y., Neal, C.A., and Okamura, A.T., 1987, The Puu Oo eruption at Kilauea, episodes 1–20, January 3, 1983, to June 8, 1984, *in* Decker, R.W., et al., eds., Volcanism in Hawaii: U.S. Geological Survey Professional Paper 1350, p. 471–508.